Macromolecular Research (2024) 32:505–513
https://doi.org/10.1007/s13233-023-00243-5

Online ISSN 2092-7673
Print ISSN 1598-5032

ARTICLE

New pyrazine-based π-conjugated polymer for dopant-free perovskite solar cell

Jeonghyeon Park[1] · Lakshman Chetan[1] · Hyerin Kim[1] · Je-Sung Jee[1] · Yeong-Soon Gal[2] · Sung-Ho Jin[1]

Received: 6 October 2023 / Revised: 8 December 2023 / Accepted: 17 December 2023 / Published online: 8 April 2024

Abstract

The polymer was engineered and synthesized for the fabrication of perovskite solar cells (PSCs). Pyrazine-based polymer is used as a hole transport material (HTM) in PSCs. Pyrazine is suitable for major transport, such as affording high hole mobility and intermolecular enhancement, and has the advantage of being inexpensive. Remarkable results are achieved by polymerizing a pyrazine-based material (PzTBr) composed of thiophene moiety with a short alkyl group on both sides and a BDT-based material (BDTEH) to yield BDTEH–PzTBr. Dopant-free processed PSCs fabricated with BDTEH–PzTBr exhibited a PCE of 13.2% for green solvent and 15.9% for chloroform solvent. Therefore, the pyrazine-based polymer is an appropriate strategy to synthesize and explore as an HTM in PSCs.

Graphical abstract

A donor–acceptor (D–A)-conjugated polymer BDTEH–PzTBr was designed and successfully used as a hole transport material in perovskite solar cells. Due to the advantage of the molecular structure, and uniform morphology, the BDTEH–PzTBr-based device achieved a good power conversion efficiency of over 15.9%. High performance is achieved using easy synthesis processes and inexpensive materials.

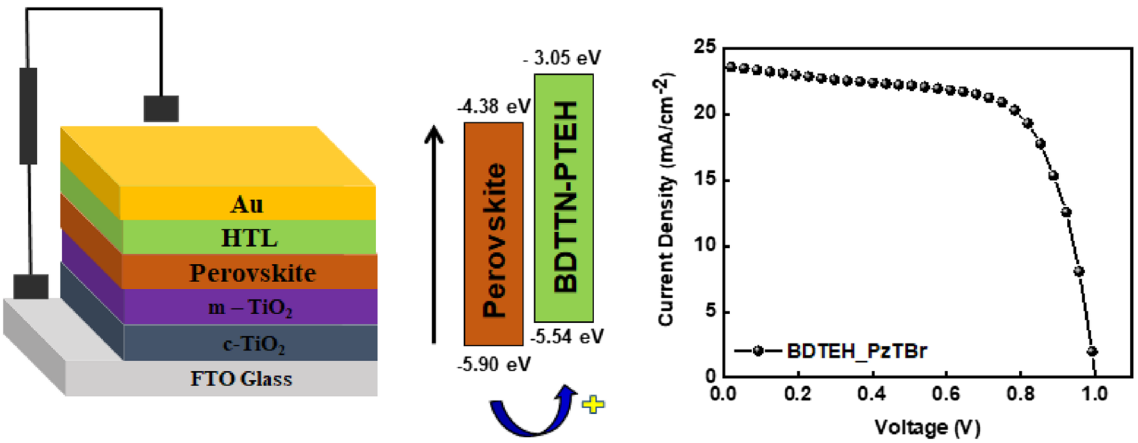

Keywords Benzodithiophene · Perovskite solar cell · Pyrazine · Hole transport material · Dopant-free

1 Introduction

Perovskite solar cells (PSCs) appeared as a latecomer in the solar cell field; thanks to their low-cost materials, components, simple solution fabrication process, broad light absorption, efficient charge-transfer ability, long carrier diffusion lengths, and tunable bandgap. Initiated in 2009 with a power conversion efficiency (PCE) of 3.8%, PSCs have seen a rapid growth of nearly 26% in less than two decades. For this reason, PSCs are attracting great attention and are suitable for the next generation solar cell [1–5].

Extended author information available on the last page of the article

Hole transport materials (HTMs) have a major effect on the performance of PSCs. Other crucial PSCs material components were produced by researchers to further enhance performance, such as electron-transporting layers (ETLs), hole-transporting layers (HTLs), and counter electrodes. Among these, HTM materials applied to HTL have been studied by researchers. Currently, the conventional HTM 2,2′,7,7′-tetrakis [N,N-di(4-methoxyphenyl)amino]-9,9′-spirobifluorene (Spiro-OMeTAD) along with dopants like lithium bis(tri-fluoromethanesulfonyl)imide (Li-TFSI) and 4-*tert*-butyl pyridine (*t*BP) was used to achieve the highest PCE in PSC's. However, the hygroscopic Li-TFSI and volatile tBP deteriorate the HTM films by absorbing moisture, affecting the charge-transfer process. As a result, moisture intercalation decomposes the perovskite layer and decreases the performance and device stability [6–8]. Dopant-free HTMs have the potential to address the adverse stability issue with perovskite solar cells. Lately, some dopant-free HTMs have produced robust PSCs with efficiencies above 20% [9]. Donor–acceptor (D–A) polymers have outstanding hole-transporting characteristics and significant light absorption from conjugated rings due to an internal charge-transfer mechanism. As a result, D–A polymers are promising dopant-free HTM options for traditional n-i-p PSCs. Modulation of the D–A units can greatly alter the band-gaps, carrier mobilities, and energy levels of D–A polymers [10, 11]. To adjust the optoelectronic properties of PSCs, benzo[1,2-b:4,5-b]dithiophene (BDT) was chosen for its planar conjugated structures and exceptional hole mobility. Changing the alkyl chain on BDT improves solubility, solution processing, and device film [12]. Gururaj et al. incorporated the pyrazine molecule as an acceptor molecule for the first time. Herein, a single aromatic heterocycle, pyrazine has a π-conjugation character and high polarizability. This guarantees a deep HOMO level in relation to the high V_{oc} value in the PSCs because of the good electron-withdrawing impact of pyrazine [13]. The current study is entrenched in synthesizing core group-engineered HTMs based on the aforementioned merits. For this reason, pyrazine moiety is suitable for designing a polymer material applied to HTL.

Herein, a BDT-pyrazine-based conjugated polymer, poly[2-(5-(4,8-bis((2ethylhexy l)oxy)-6-methylbenzo[1,2-b:4,5-b′]dithiophen-2-yl)-4-(2-ethylhexyl)thiophen-2-yl)-5-(4-(2-ethylhexyl)-5-methylthiophen-2-yl)pyrazine] (BDTEH–PzTBr) was designed and synthesized. This material was processed by blending with green solvents, 2-MA and *o*-Xylene, resulting (showing) a PCE of 13.3%. To obtain good performance, chloroform was processed as a solvent, and V_{oc} and FF were measured along with the solubility of the material and the PCE increased to 15.9%.

2 Experimental

2.1 General information

2,5-Dibromopyrazine was obtained from Sigma Aldrich (Korea), benzo[1,2-b:4,5-b]dithiophene-4,8-dione was purchased from Alfa chem. (Korea). Our previous procedures were followed to synthesize the monomers and ^{1}H NMR was used to confirm them. Monomer 1 was synthesized according to a previous report (Scheme 1) [14].

2.2 Synthesis of materials synthesis of 3-(2-ethylhexyl)thiophene (1)

3-bromothiophene (2 g, 12.22 mmol) was added in 50 ml two-neck round bottom flask under a nitrogen condition, thereafter 20 mL of anhydrous tetrahydrofuran was injected and stirred under N_2 atmosphere for 10 min. [1,3-Bis(diphenylphosphino)propane]dichloronickel (II) (0.066 g, 0.12 mmol) was inserted quickly and purged until the two-neck round bottom flask was filled with N2 conditions. 2-ethyl hexyl magnesium bromide (3.2 g, 14.72 mmol)

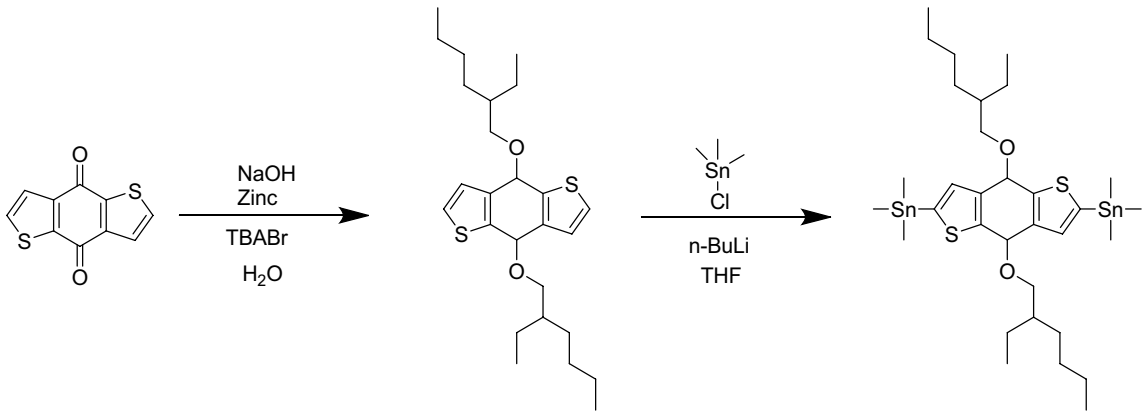

Scheme 1 Synthetic routes of the monomer 1

was added into the flask. The mixture was refluxed at 75 °C and stirred overnight in an oil bath.

Water was used to quench the reaction, dichloromethane to extract it, and anhydrous sodium sulfate was used to dry it. Following the removal of the organic layer, the product was processed using column chromatography with hexane as an eluent., compound **1** as a colorless oil [15] (1.95 g, Yield: 81%). ^{1}H NMR (400 MHz, $CDCl_3$) δ 7.26–7.24 (dd, 1H), 6.94–6.92 (dd, 1H), 2.59 (d, 2H), 1.73–1.59 (m, 1H), 1.34–1.21 (m, 8H), 0.91–0.84 (m, 6H).

2.2.1 Synthesis of tributyl(4-(2-ethylhexyl)thiophen-2-yl) stannane (2)

In 50 ml 2-neck round bottom flask, compound 1 (1 g, 5.09 mmol) was dissolved in 15 ml anhydrous THF under N_2 conditions. The TMEDA (1.143 mL, 7.64 mmol) was injected at − 78 °C. After 10 min, the n-BuLi (2.5 M in hexanes, 3.259 mL, 8.15 mmol) was added to the flask dropwise and stirred for 1.5 h. Tributyltin chloride (2.072 mL, 7.64 mmol) was added dropwise within 10 min to the flask and stirred for 2 h. Distilled water (DI) was used to dilute the mixture, which was subsequently separated with dichloromethane and anhydrous sodium sulfate was used to dry it. The mixture was dried without any purification after evaporating the organic layer. Compound **2** as a yellow oil.

2.2.2 Synthesis of 2,5-bis(4-(2-ethylhexyl)thiophen-2-yl) pyrazine (3)

Tributyl(4-(2-ethylhexyl)thiophen-2-yl)stannane (0.2 g, 0.84 mmol) was added in a 50 ml two-neck round bottom flask under nitrogen conditions. 1,4-dibromopyrazine (2.45 g, 5.04 mmol) was added. Later, Tetrakis(triphenylphosphine)palladium (0.49 g, 0.04 mmol) was added under dark conditions and stirred while preventing light from entering. The reactants were heated for 24 h at 110 °C, cooled, and poured into water to be extracted with dichloromethane. On top of anhydrous Na_2SO_4, the organic layer was dried. Using silica gel chromatography and dichloromethane (30% in hexane), the crude chemical was refined. The compound obtained was a yellow solid [16, 17]. (0.38 g, yield: 97%). ^{1}H NMR (400 MHz, $CDCl_3$) δ 7.39 (s, 2H), 6.97 (a, 2H), 2.52 (d, 4H), 1.53 (s, 2H), 1.28–1.18 (m, 16H), and 0.85–0.81 (m, 12H).

2.2.3 Synthesis of 2,5-bis(5-bromo-4-(2-ethylhexyl) thiophen-2-yl)pyrazine (4) (monomer 2)

In a 25 ml round bottom flask, 2,5-bis(4-(2-ethylhexyl)thiophen-2-yl)pyrazine(0.13 g, 0.277mmol) was dissolved in 10ml of THF within nitrogen conditions. NBS (0.12 g, 0.69 mmol) was quickly added under dark conditions, sealed well to prevent light from passing through, and stirred overnight. Water was used to quench the reaction, dichloromethane to extract it, and anhydrous sodium sulfate was used to dry it. Following the removal of the organic layer, the product was processed using column chromatography with hexane: dichloromethane (4:1) as an eluent, The compound obtained was a yellow solid [18]. (0.62 g, Yield: 92%). ^{1}H NMR (400 MHz, $CDCl_3$) δ 8.66 (s, 2H), 7.23 (s, 2H), 2.47 (d, 4H), 1.59 (m, 2H), 1.29–1.24 (m, 16H), 0.86–0.82 (m, 12H) ^{13}C NMR (500 MHz, $CDCl_3$) δ 146.01, 143.61, 140.76, 139.40, 127.07, 124.29, 77.29, 77.04, 76.78, 40.32, 40.17, 34.60, 32.45, 29.72, 28.88, 25.61, 23.06, 14.16, 10.85 (Scheme 2).

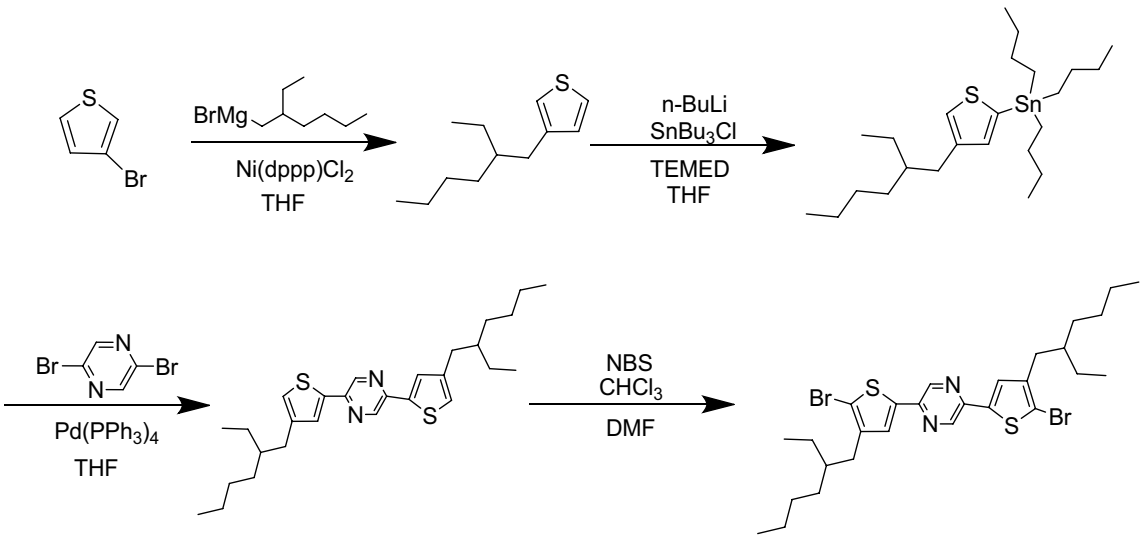

Scheme 2 Synthetic routes of the monomer 2

2.2.4 Synthesis of poly[2-(5-(4,8-bis((2-ethylhexyl)oxy)-6-methylbenzo[1,2-b:4,5-b′]dithiophen-2-yl)-4-(2-ethylhexyl)thiophen-2-yl)-5-(4-(2-ethylhexyl)-5-methylthiophen-2-yl)pyrazine]

In a 10 mL microwave tube, Monomer 1 (0.32 mmol), Monomer 2 (0.32 mmol), and anhydrous chlorobenzene (1 mL) were stirred under nitrogen conditions. After 20 min, $Pd_2(dba)_3$ (10 mol %), and $(o\text{-tol})_3P$ (20 mol %) were added. Under nitrogen conditions, the reactants were stirred for 15 min. After being inserted into the reactor, the microwave tube was heated for 1.5 h to 135 °C. After reaching room temperature, a precipitate appeared when it was poured into methanol. Later, Soxhlet extraction was used for purification. Processed in the order of methanol, hexane, acetone, and chloroform. Evaporating chloroform yielded the polymer [19]. (81%) (Scheme 3). $M_n = 34{,}351\ gmol^{-1}$, PDI = 1.26 ^{1}HNMR: 7.55–7.23 (m, 2H), 7.52–7.40 (m, 3H), 6.95–6.77 (m, 1H), 4.25–4.05 (m, 8H), 2.82 (m, 4H), 1.44–1.17 (m, 24H), 1.1–0.75 (m, 24H).

2.3 Device fabrication and measurements

2.3.1 Fabrication

FTO glass was etched and washed using H_2O_2/HCl/H_2O = 1:1:5 (RCA-2) procedure by ultrasonication for 15 min and followed by a sequential wash with CH_3COCH_3 and isopropyl alcohol. Titanium diisopropoxide bis(acetylacetonate) was dissolved in ethanol (1:10) to prepare the TiO_2 precursor and was sprayed onto the FTO at 450 °C to form the c-TiO_2 layer. Next, the substrates were heated at 450 °C for 60 min. m-TiO_2 (TiO_2 paste dissolved in 2-ME/terpineol) was spin-coated on the c-TiO_2 layer at 3000 rpm for 50 s and was heated at 500 °C on a hotplate for 60 min. Next, Li-TFSI solution (0.5 mg/1 mL of acetonitrile) was spin-coated on the TiO_2 and heated at 500 °C for 60 min. The perovskite precursor solution was made by dissolving 775 mg $CsFAPbI_3$, 30 mg MACl, and 6 mg $MABr_3$ with 0.5 mL DMF/DMSO (4:1). The perovskite solution was spun at 8000 rpm for 50 s, after 10 s 1 mL diethyl ether was dropped on the substrate. The film was annealed on a hotplate for 10 min at 150 °C. Passivator 4-fluorobenzamide hydrochloride (FPhFACl) was coated at 3000 rpm for 30 s on the perovskite layer. BDTEH–PzTBr polymer HTM (10 mg/mL) was spun at 5000 rpm for 30 s. Lastly, the gold (Au) electrode (60 nm) was deposited thermally on the HTM.

3 Results and discussion

The polymerization process was carried out under microwave conditions, as shown in Scheme 3. Using ^{1}H NMR spectroscopy, the polymer and all intermediates were identified. The molecular weight of the polymer was calculated via gel permeation chromatography (GPC) as ($M_n = 34{,}351\ gmol^{-1}$, PDI = 1.43). Thermal, electrochemical, and photophysical properties are recapitulated in Table 1. Figure 1a shows the UV–vis absorption spectra of BDTEH–PzTBr in a dilute CF solution. A significant absorption band at roughly 450–600 nm results in the intramolecular charge transfer between the BDT molecule and the pyrazine moiety. BDTEH–PzTBr exhibited maximum absorption at

Table 1 Thermal, electrochemical, and photophysical properties of polymer

Polymer	Film[a] λ_{max} [nm]	T_d[b] [°C]	HOMO[c] (eV)	LUMO[d] (eV)	E_g[e] (eV)
BDTEH–PzTBr	498	385	− 5.54	− 3.05	2.49

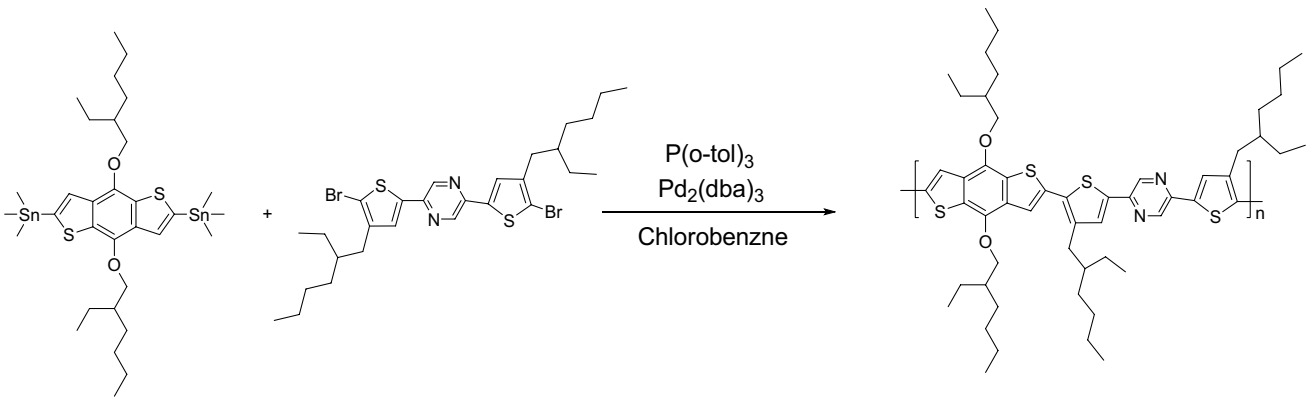

Scheme 3 Synthetic routes of the BDTEH–PzTBr

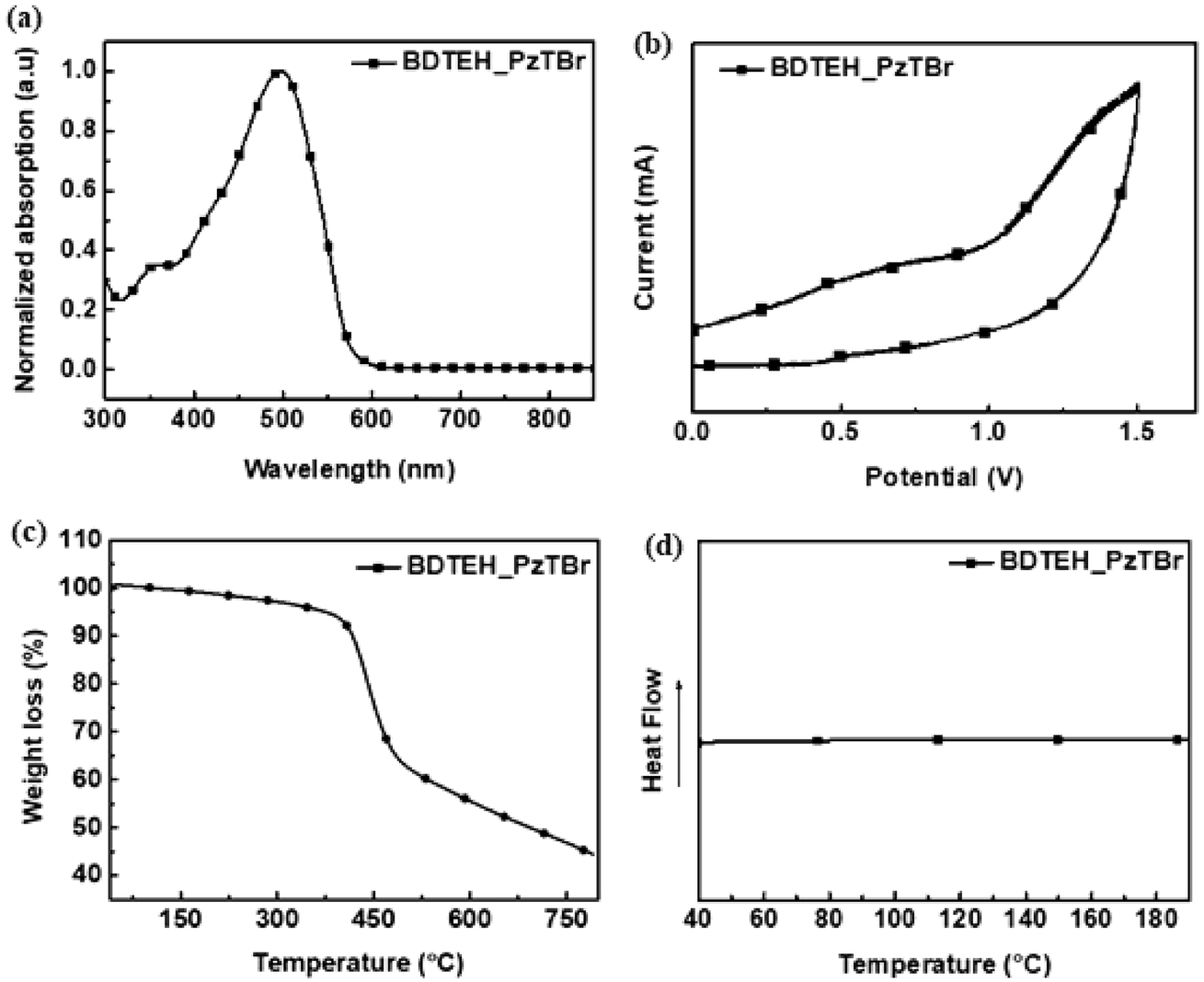

Fig. 1 **a** UV–vis absorption spectra in film state **b** CV **c** TGA and **d** DSC measurement

495–501 nm and a weak absorption at 350 nm, indicating strong interchain π–π* absorption. Based on UV data, the energy band gap (Eg) of BDTEH–PzTBr is estimated which is (E_{gopt} = 2.49 eV). The BDTEH–PzTBr energy levels were estimated using the cyclic voltammetry (CV) depicted in Fig. 1b. The HOMO energy level was calculated using the formula HOMO (eV) = − ($E_{ox\ Offset}$ + 4.8 − $E_{ox,\ Ferrocene}$) and found to be − 5.54 eV. LUMO (eV) = HOMO (eV) + $E_{g\ opt}$. was calculated according to the empirical formula listed below to derive the value [20, 21]. Table 1 summarizes the relevant values. To examine the thermal characteristics, differential scanning calorimetry (DSC) and Thermal gravimetric analysis (TGA) were employed. Figure 1c shows that 385 °C was determined to be the decomposition temperature (Td, which corresponds to a 5% weight loss). The DSC curve indicates that no heat absorption peak was seen at that specific temperature range (Fig. 1). These findings reveal that the produced polymer has good thermal stability. The molecular structures of BDTEH–PzTBr, acceptor PzTBr, and donor BDTEH are shown in Fig. 2a–c, respectively. Figure 2d provides an accurate representation of the PSC architecture and the energy level diagram which demonstrates that the BDTEH–PzTBr has great energy levels needed for superior photovoltaic device performance. We developed perovskite solar cells with conventional FTO/c-TiO_2/mp-TiO_2/Perovskite/HTM/Au configuration to test the efficacy of BDTEH–PzTBr polymer as a dopant-free HTM. The photovoltaic performance is illustrated in Table 2.

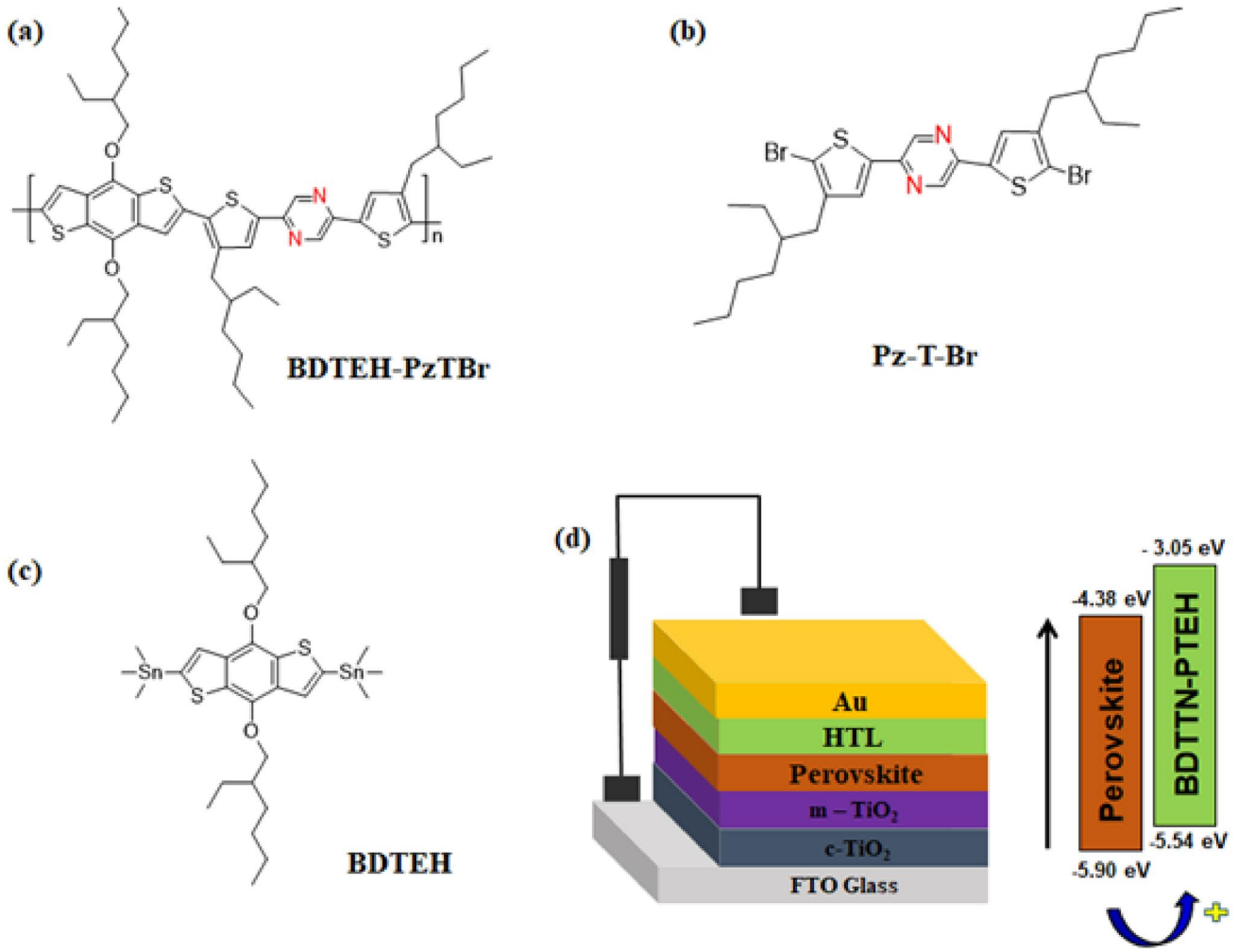

Fig. 2 Molecular structure of **a** BDTEH–PzTBr **b** BDTEH **c** PzTBr **d** device configuration and energy level diagram

Table 2 Photovoltaic performance of BDTEH–PzTBr-based OSCs processed with solvent

Devices	D:A (ratio)	Solvent	V_{oc} (V)	J_{sc} (mAcm^{-2})	FF (%)	PCE (%)
1	1:1	O-xylene/2-MA	0.90	25.68	57.73	13.3
2	1:1	Chloroform	0.99	23.51	67.73	15.9

Initially, the BDTEH–PzTBr polymer exhibited a PCE of 13.3% with J_{sc} of 25.6 mA cm^2, V_{oc} of 0.90 V, FF of 57.7% when checked with 2-methyl anisole (2-MA) a green solvent. But, chloroform (CF) solvent exhibited good solubility and yielded a good PCE of 15.9% with J_{sc} of 23.5 mA cm^2, V_{oc} of 0.99 V, FF of 67.7%. External quantum efficiency (EQE) was investigated to estimate the integrated J_{sc}. The integrated J_{sc} of BDTEH–PzTBr polymer-based perovskite device is 22.6 mA cm^{-2} and is an excellent match for the experimental result [22]. The unencapsulated device could maintain 76% of its initial PCE after 300 h in ambient air depicting good stability (Fig. 3c). Additionally, atomic force microscopy (AFM) was performed to investigate the surface morphology of the perovskite and HTM [23]. The roughness root mean square (RMS) value for perovskite is 41 nm and after coating the HTM it reduced to 29 nm, showing that the uniform coating of BDTEH–PzTBr on the perovskite layer is advantageous in terms of safeguarding the perovskite from moisture, ensuring good stability, and lowering detrimental shunt losses [24] (Fig. 4). In addition to this, neat perovskite showed a contact angle of 78.6°, and the HTM-coated perovskite showed a greater contact angle of 97.7° providing good stability and moisture resistance [25] (Fig. 5).

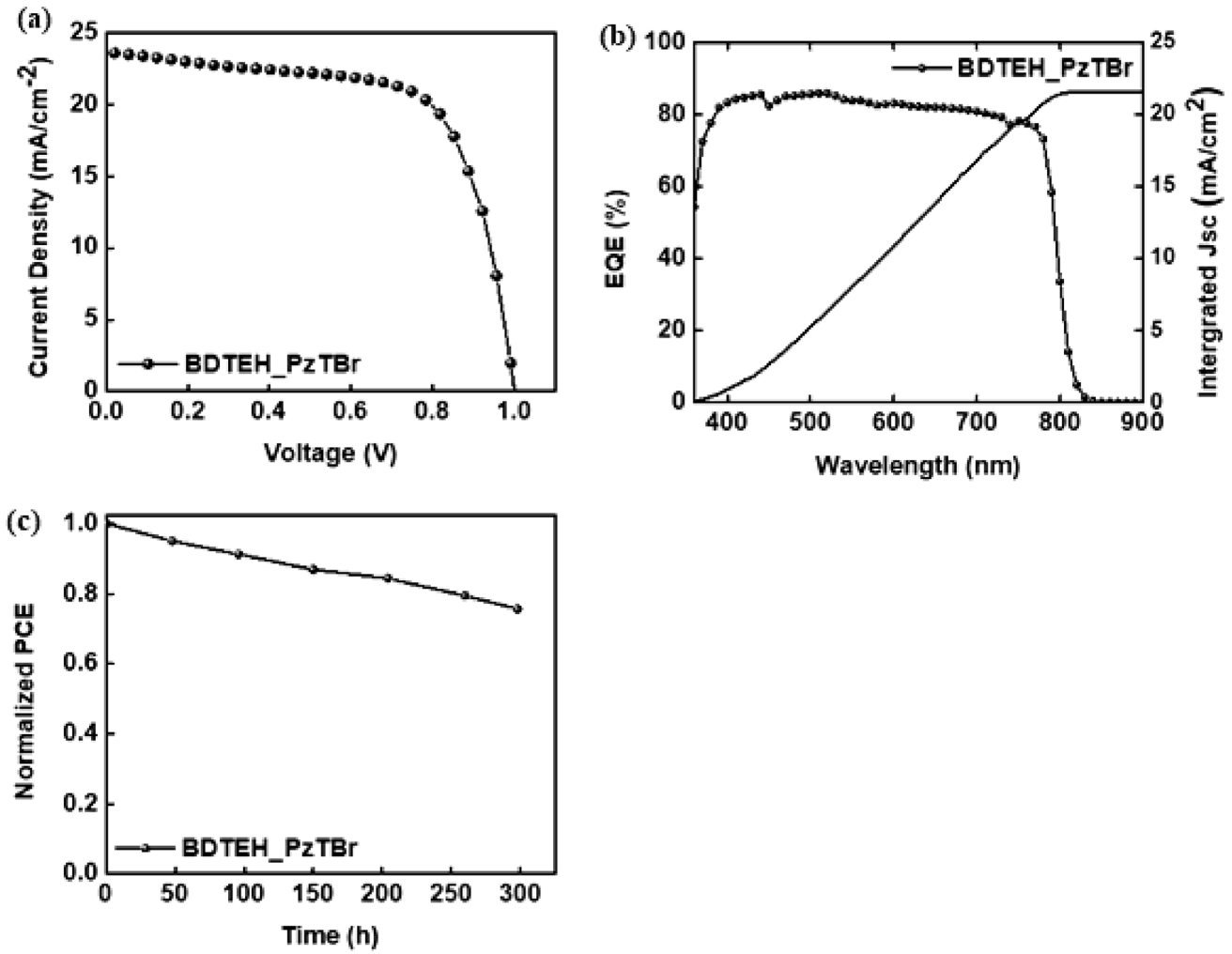

Fig. 3 **a** J–V curve of BDTEH–PzTBr **b** EQE spectra of BDTEH–PzTBr-based PSCs **c** stability study of BDTEH–PzTBr

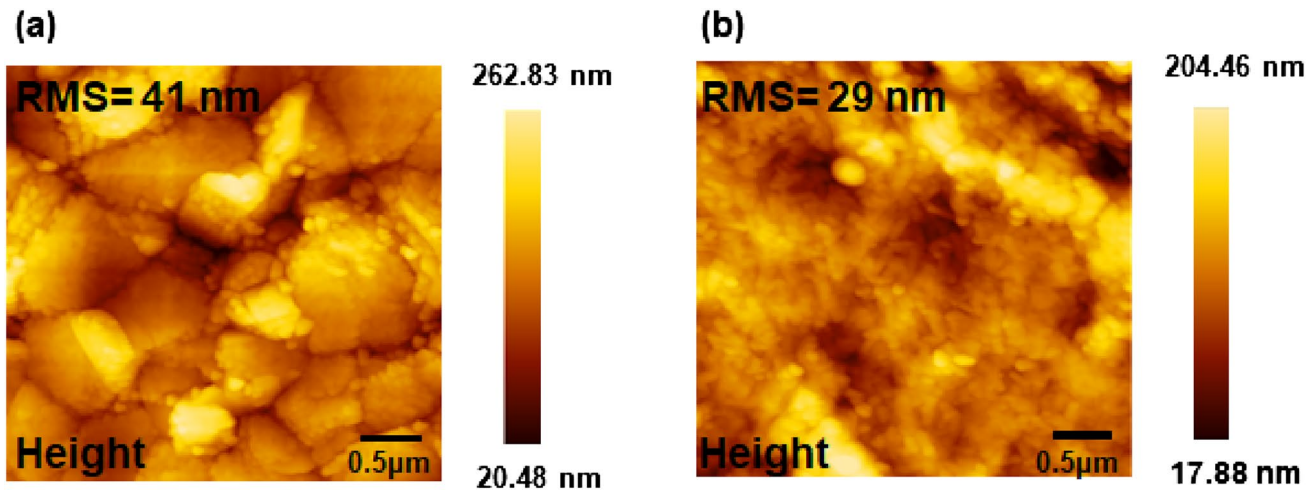

Fig. 4 AFM images film **a** perovskite height and **b** perovskite, HTM height, respectively

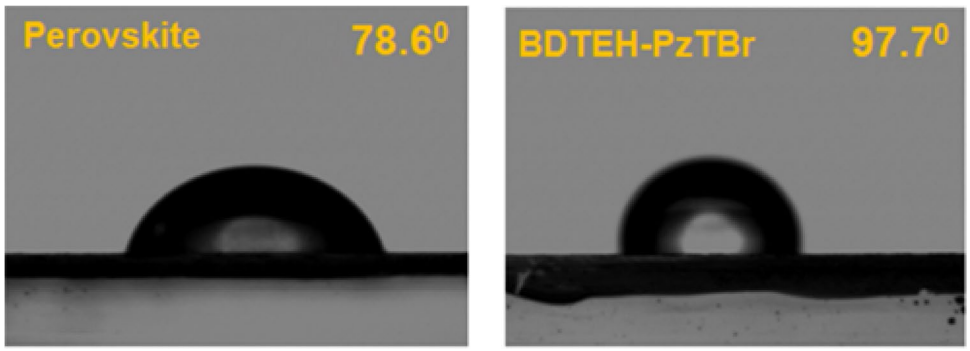

Fig. 5 Contact angle studies

4 Conclusions

In conclusion, a polymer based on pyrazine (BDTEH–PzTBr) was synthesized and used in the fabrication of solvent-processed PSCs. The green solvent o-xylene/2-MA processed device achieved a PCE of 13.3% with J_{sc} of 25.6 mA cm^2, V_{oc} of 0.90 V, FF of 57.7%. Using chloroform as a solvent the dopant-free PSC achieved an impressive PCE of 15.9% with J_{sc} of 23.5 mA cm^2, V_{oc} of 0.99 V, and FF of 67.7%. These results support that, pyrazine-based polymers are suitable for morphological improvement and have outstanding hydrophobic properties. Pyrazine-based polymer synthesis has been shown to be an effective and promising method for creating high performance for the PSCs [26].

Acknowledgements J. Park and L Chetan contributed equally to this work. This research was funded by a two-year Research Grant of Pusan National University.

Author contributions JP, HK, LC: conceptualization, methodology, formal analysis, writing—original draft. J-SJ, Y-SG, S-HJ: writing—review and editing, supervision, project administration, funding acquisition.

Declarations

Conflict of interest The authors declare that they have no known competing financial interests or personal relationships that could have appeared to influence the work reported in this paper.

References

1. R.D. Gayathri, C. Lakshman, H. Kim, J. Park, D. Song, J. Lee, H.Y. Park, R. Kumaresan, T. Gokulnath, S.H. Jin, ACS Appl. Mater. Interfaces **15**, 31514 (2023)
2. X. Liu, S. Fu, W. Zhang, Z. Xu, X. Li, J. Fang, Y. Zhu, A.C.S. Appl, Mater. Interfaces **13**, 52549 (2021)
3. Z.Z. Sun, R. Long, Chem. C **27**, 12913 (2023)
4. C. Yi, K. Yue, W.B. Zhang, X. Lu, J. Hou, Y. Li, L. Huang, G.R. Newkome, S.Z.D. Cheng, X. Gong, A.C.S. Appl, Mater. Interfaces **6**, 14189 (2014)
5. S.N. Afraj, M.H. Lin, C.Y. Wu, A. Velusamy, P.Y. Huang, T.Y. Peng, J.C. Fu, S.H. Tung, M.C. Chen, C.L. Liu, J. Mater. Chem. C **10**, 14496 (2022)
6. Y. Rong, Y. Hu, A. Mei, H. Tan, M.I. Saidaminov, S.I. Seok, M.D. McGehee, E.H. Sargent, H. Han, Science **361**, 6408 (2018)
7. T. Zhang, X. Wang, M. Kan, J. Shi, Y. Zhao, Angew. Chem. **131**, 16844 (2019)
8. Z. Xie, H. Park, S. Choi, H.-Y. Park, T. Gokulnath, H. Kim, J. Kim, H.-B. Kim, I.W. Choi, Y. Jo, D.S. Kim, Y.-Y. Yoon, S.-Y. Yoon, J. Yoon, Y.-R. Cho, S.-H. Jin, Adv. Energy Mater. **13**, 2202680 (2023)
9. L. Zhou, L. Meng, J. Zhang, C. Zhu, S. Qin, I. Angunawela, Y. Wan, H. Ade, Y. Li, Adv. Funct. Mater. **32**, 2109271 (2022)
10. S.N. Afraj, D. Zheng, A. Velusamy, W. Ke, S. Cuthriell, X. Zhang, Y. Chen, C. Lin, J.S. Ni, M.R. Wasielewski, W. Huang, J. Yu, C.H. Pan, R.D. Schaller, M.C. Chen, M.G. Kanatzidis, A. Facchetti, T.J. Marks, ACS EnergyLett. **7**, 2118 (2022)
11. G. You, Q. Zhuang, L. Wang, X. Lin, D. Zou, Z. Lin, H. Zhen, W. Zhuang, Q. Ling, Adv. Energy Mater. **10**, 1903146 (2020)
12. J. Hai, W. Yu, Z. Baofeng, Y. Li, L. Yin, E. Zhu, B. Linyi, J. Zhang, H. Wu, W. Tang, Polym. Chem. **5**, 1163 (2014)
13. G.P. Kini, J.Y. Choi, S.J. Jeon, I.S. Suh, D.K. Moon, Polym. Chem. **10**, 4459 (2019)
14. P. Morvillo, F. Parenti, R. Dianna, C. Fontanesi, A. Mucci, F. Tassinari, L. Schenetti, Sol. Energy Mater. Sol. Cells, **104**, 45 (2012)
15. H. Yao, L. Ye, H. Zhang, S. Li, S. Zhang, J. Hou, Chem. Rev.v. **12**, 7397 (2016)
16. K. Chen, X. Deng, G. Dodekatos, H. Tüysüz, J. Am. Chem. Soc. **35**, 12267 (2017)
17. S. Hu, X. Bao, Z. Liu, W. Ting, Z. Du, S. Wen, N. Wang, L. Han, R. Yang, Org. Electron. **12**, 3601 (2014)
18. E.H. Park, J.J. Ahn, H.S. Kim, J.H. Kim, D.H. Hwang, J. Korean Chem. Soc. **3**, 196 (2016)
19. L. Zhou, X. Xia, L. Meng, J. Zhang, X. Lu, Y. Li, Chem. Mater. **33**, 8212–8222 (2021)
20. C.Y. Hsiow, R. Raja, C.Y. Wang, Y.H. Lin, Y.W. Yang, Y.J. Hsieh, S.P. Rwei, W.Y. Chiu, C.I. Huang, L. Wang, Phys. Chem. Chem. Phys. **16**, 25111 (2014)
21. R.D. Gayathri, Y. Do, J. Kim, H. Kim, T. Gokulnath, Y.S. Gal, S.H. Jin, Mol. Cryst. Liq. Cryst. **1**, 11 (2022)
22. H. Wang, J. Gao, L. Gu, J. Wan, W. Wei, F Liu J. Mater. Chem. A **1**, 5875–5885 (2013)
23. S.J. Nam, S.J. Jeon, Y.W. Han, D.K. Moon, J. Ind. Eng. Chem. **63**, 191 (2018)
24. X. Jiang, J. Zhang, Y. Liu, Z. Wang, X. Liu, X. Guo, C. Li, Nano Energy **90**, 106521 (2021)
25. Z. Xie, Y. Do, S.J. Choi, H.Y. Park, H. Kim, J. Kim, D. Song, T. Gokulnath, H.B. Kim, I.W. Choi, Y. Jo, D.S. Kim, S.Y. Yoon, Y.R. Cho, S.H. Jin, Mater. Chem. A **11**, 9608 (2023)

26. J. Hai, W. Yu, E. Zhu, L. Bian, J. Zhang, W. Tang, Thin Solid Films **562**, 75 (2014)

Authors and Affiliations

Jeonghyeon Park[1] · Lakshman Chetan[1] · Hyerin Kim[1] · Je-Sung Jee[1] · Yeong-Soon Gal[2] · Sung-Ho Jin[1]

✉ Je-Sung Jee
jsjee68@hanmail.net

✉ Yeong-Soon Gal
ysgal@kiu.ac.kr

✉ Sung-Ho Jin
shjin@pusan.ac.kr

[1] Department of Chemistry Education, Graduate Department of Chemical Materials, Institute for Plastic Information and Energy Materials, Sustainable Utilization of Photovoltaic Energy Research Center, Pusan National University, Busan 46241, Republic of Korea

[2] Department of Fire Safety, Kyungil University, Gyeongsan, Gyeongsangbuk-do 38428, Republic of Korea